diffusion-fundamentals.org
The Open-Access Journal for the Basic Principles of Diffusion Theory, Experiment and Application

New Instrumental Platform for the Exploitation of the Field-Dependence of T_1 in Rock Core Analysis and Petroleum Fluids : Application to T_1-T_2 Correlation Maps

Jean-Pierre Korb,[1] *Gianni Ferrante*,[2] *Salvatore Bubici*,[2] *Mike Mallett*[3]

[1] Physique de la Matière Condensée, Ecole Polytechnique-CNRS, 91128 Palaiseau, France
[2] Stelar, Via E. Fermi 4, 27035 Mede (PV) Italy
[3]HTS-110 69 Gracefield Road PO Box 31-310 Lower Hutt 5040-New Zealand

Corresponding author: Jean-Pierre Korb, Physique de la Matière Condensée, Ecole Polytechnique-CNRS, 91128 Palaiseau, France, E-Mail : jean-pierre.korb@polytechnique.fr

Abstract

We propose using the latest wide bore fast field cycling NMR relaxometers for measuring the nuclear magnetic relaxation dispersion (NMRD) profiles of the logarithmic average proton-water $<1/T_1>$ in carbonate rock cores samples of 1 inch diameter and in different crude oil/brine mixings. The observed bilogarithmic frequency behaviours of the NMRD have been interpreted with a proposed theoretical model yielding a measurement of the water local wettability at the pore surface. We have also proposed a NMR platform that uses a variable wide-bore cryogen-free superconducting magnet to acquire *2D* T_1-T_2 correlation spectrum of a mixing of bulk water and crude oil pools. Such a T_1-T_2 plot allows quantitative separation of mixed bulk water and crude oil. The *2D* plot does not reveal any exchange between the different and independent pools.

Keywords

Relaxation, T_1, T_1-T_2 correlation plot, rock-core, oil, water

1. Introduction

Recent NMR works demonstrate that Fast Field Cycling (FFC) NMR and multi-frequency NMR relaxometry offer unique insights for the study of rock cores and heavy crude oils [1-5]. Nuclear Magnetic Relaxation Dispersion (NMRD) profiles, acquired through FFC NMR relaxometry by scanning a wide range of magnetic fields, provide unique information on the surface dynamics of confined petroleum fluids in porous rocks, thus information on "wettability" in carbonates and sandstones can be obtained. T_1 distribution dispersions of crude oils as a function of the relaxation field is a powerful new technique to study asphaltene aggregation not only in model systems, but directly in heavy crude oils of various compositions [2, 3]. Such information, obtained only with the FFC NMR technique, provides important insights into highly complex fractions of crude oil and the related

aggregation phenomena [2, 3]. In petro-physical contexts, knowledge of the field/frequency dependence of relaxation can improve interpretation of T_1 and T_2 measurements in common oilfield uses, assess wettability of water in reservoir rocks and improve characterization of asphaltene aggregates (allowing oilfield operations to avoid asphaltene related problems) [4,5].

Here, we present the first NMRD data obtained with the latest wide bore fast field cycling NMR relaxometers for probing the dynamics of water in a whole set of carbonate rock-cores samples of representative sizes (1 inch diameter). The NMRD method has been also used from a few KHz up to 40 MHz to distinguish quantitatively crude oil from the response of water in different crude oil/brine mixings. Last, we present a NMR platform that uses a variable wide-bore cryogen-free superconducting magnet to acquire *2D* T_1-T_2 correlation spectrum of a mixing of bulk water and crude oil pools. Such a T_1-T_2 plot allows quantitative separation of mixed bulk water and crude oil.

2. Experiments

2.1 Samples and New Rock-Core Analyzer

For a long time, an important demand of industrial partners on FFC relaxometry was to drastically enlarge the size of the sample studied. This is indeed the case for petroleum industry where the usual rock cores reach 1 inch in diameter. The introduction of the latest Wide Bore Fast Field Cycling NMR relaxometers in the form of a 0.5 Tesla wide-bore magnet has been introduced for studying large samples of 1 inch sizes. This allows us to study, for the first time, the dynamics of confined surface water contained in the pores of rock-cores of representative sizes (1 inch in diameter and height). A 40 mm bore FFC magnet with a 0.45 Tesla maximum polarizing field was used (Fig. 1a, b). This method proved useful to study three different carbonate rock samples labeled S40, S50, S122 of 25 mm diameter and 20 mm height, with different porosities and saturated with de-ionized water (Fig. 1c). This facilitates the interpretation of the NMRD data because the water viscosity and diffusivity do not depend on the brine salinity.

(a) **(b)** **(c)**

Fig. 1: (a) Large volume probe. **(b)** SPINMASTER Wide Bore FFC magnet, internal bore 40 mm, maximum field 0.45 Tesla. **(c)** Three samples of carbonate rocks measuring 25 mm in diameter and 20 mm in height

2.2. ESR of Carbonate Rock-Cores

We use the X-band ESR spectra for characterizing the paramagnetic relaxation sinks in the three rock-cores. These ESR data were taken such as the central peaks were not saturated or did not overload the receiver. We fix the center magnetic field at 325.99 mT and sweep the field from 175 to 476 mT. The nominal microwave power was 2.00 mW and we use a 100 kHz modulation frequency with a 0.1 mT modulation amplitude. We accumulate each signal three times. The six-peak hyperfine structures of the ESR spectrum displayed in Fig. 2 for the three rock-cores are identical and typical of Mn^{2+} ions (S=5/2) convoluted by a power pattern.

diffusion-fundamentals.org 22 (2014) 5, pp 1-7

We note differences of intensities in these ESR spectra. So, a true calibration of the ESR data is needed for obtaining the density η_S of paramagnetic ions Mn^{2+} per gram of dry material (rock-core). We have proposed a calibration-method comparing the surface area of all the rock-ESR signals with the one of a definite amount of CuSO4 diluted in an inert KBr powder free of paramagnetic impurities. This method gives η_S = 1.06, 2.83 and 2.90 10^{18} Mn^{2+}/g, for the three samples S40, S50 and S122, respectively. Assuming a uniform distribution, we can deduce a surface density of Mn^{2+} impurities, $\sigma_S \approx (\eta_S \rho_{rock})^{2/3}$ of the order {2.06, 3.88 and 3.94 10^{12} Mn^{2+}/cm^2} where $\rho_{rock} \approx 2.7\ g/cm^3$ is the average density of the rocks.

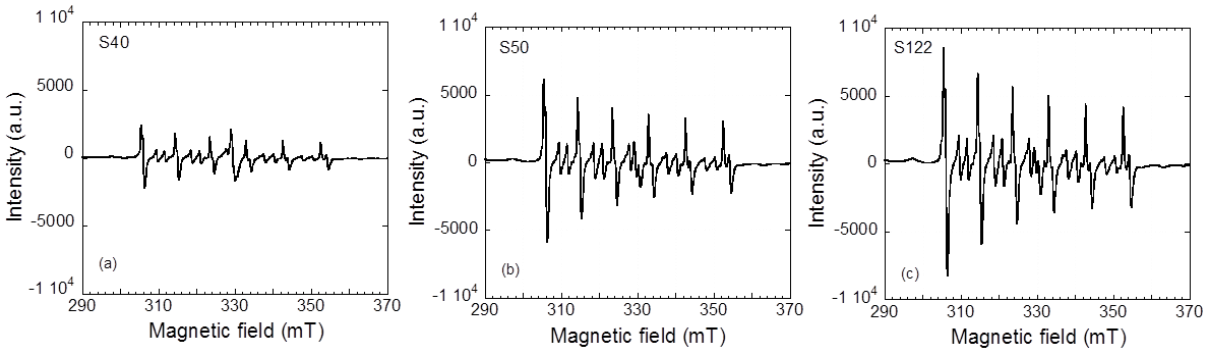

Fig. 2 Electron spin resonance spectra of the three carbonate rock-cores studied.

2.3. Proton T_1-Distribution of Water in Carbonate Rock-Cores at Different Frequencies

We present in Figs. (3a-c), the resulting stack plots of the water-proton T_1 distributions obtained, with an inverse Laplace transform (ILT) of the longitudinal magnetization decays of the three rock cores, and measured over the whole frequency range.

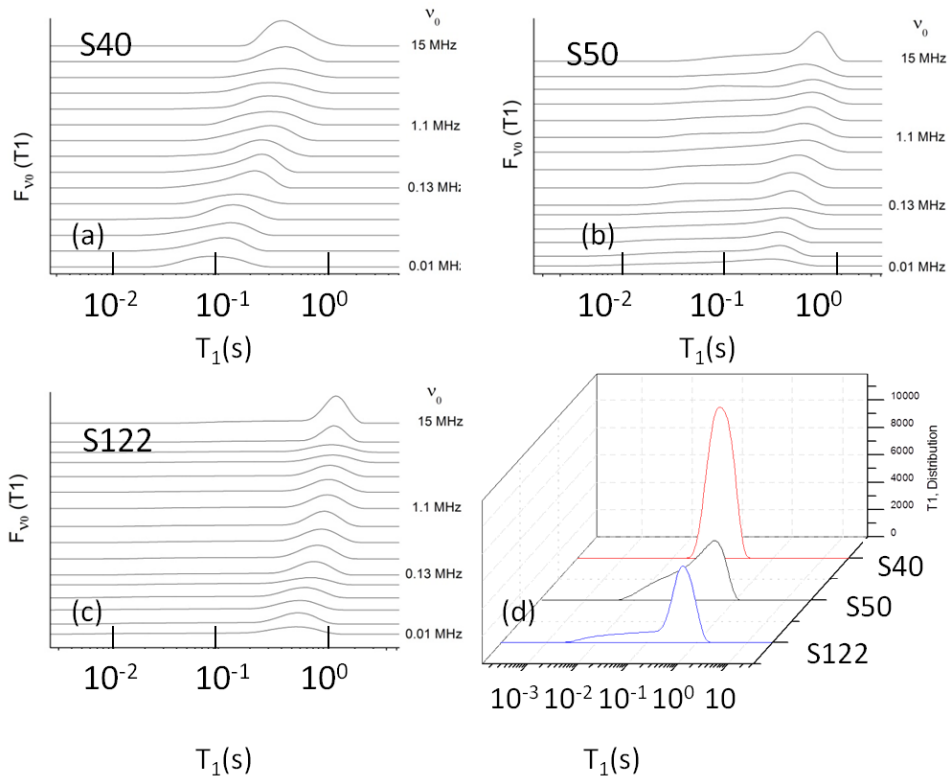

Fig. 3 (a-c) Stack-plots of the T_1-distributions of three rock-cores represented at different frequencies.
(d) Comparison of the three T_1-distributions represented at a given frequency ν_0=0.01 MHz.

In all the cases, we note a very large T_1 distribution where it is really difficult to discriminate any bimodal distribution. In the water-wet condition of our samples T_1 is proportional to the volume to surface ratio of the pores. So, the origin of the broad T_1-distributions reflects the distribution of pore sizes. In Fig. 3d, we evidence, at the lowest frequency ν_0=0.01 MHz, different forms of the T_1 distributions for the three rock-cores samples. Moreover, we observe a significative shift of the main peak to the small T_1 values when lowering the frequency ν_0.

3. Results and Discussion of NMRD Profiles of Water in Carbonate Rock-Cores

For creating NMRD profiles representative of the broad T_1 distributions, we calculate from the Figs (3a-d), the logarithmic average proton-water longitudinal relaxation rate defined as $\left\langle 1/T_1(\omega_I)\right\rangle = \exp\left(-\sum_{i=1}^{n} f_i \ln T_{1,i}(\omega_I)\right)$ where f_i is the i^{th} value of the discretized T_1 distribution at angular frequency ω_I. We interpret the bilogarithmic frequency behaviors of the NMRD profiles observed for the three samples (Fig. 4a) in terms of our previously proposed model of NMRD in porous media when a large number of protons (I) spin–bearing water molecules diffuse in pores with a surface density σ_S of fixed paramagnetic impurities of spins (S) [6, 1]. The bilogarithmic behavior in Fig. 4a strongly suggests the hypothesis of a *2D* diffusion of a proton-water spins *I=1/2* in the dipolar field of the fixed paramagnetic impurities *S=5/2* (for Mn^{2+}) at proximity of the flat lamellar mineral pore surface. This dynamics modulates the intermolecular dipole-dipole interaction between the moving I proton bearing oil species and the fixed S paramagnetic spins of Mn^{2+} at the pore surface. The logarithmic behaviour is due to the reduced dimensionality of the local dynamics that enhances drastically the reencounter probability between I and S spins and maintains at long-time (low frequency) the pairwise dipolar correlation between these two spins [1, 3, 6]. In the fast diffusion limit where the exchange time between the surface and the bulk phases is shorter than their respective relaxation times, the proton relaxation rate $R_{1,water}$ is a linear combination of a bulk $(R_{1,bulk})$, and a frequency-dependent contribution coming from the 2D diffusion of water molecules in proximity of the pore surface [1, 6]:

$$R_{1,water}(\omega_I) = R_{1,bulk} + C\,\tau_m\left[3\ln\left(\frac{1+\omega_I^2\tau_m^2}{(\tau_m/\tau_s)^2+\omega_I^2\tau_m^2}\right)+7\ln\left(\frac{1+\omega_S^2\tau_m^2}{(\tau_m/\tau_s)^2+\omega_S^2\tau_m^2}\right)\right] \quad (1)$$

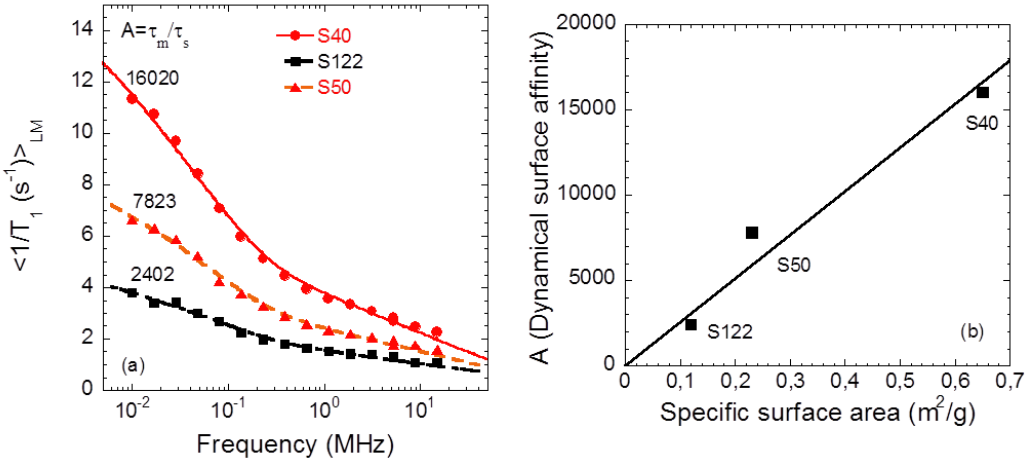

Fig. 4 (a) Nuclear magnetic relaxation dispersion of the logarithmic average $<1/T_1>$ of the rock-cores: S40, S122 and S50. The continuous lines are the best fits obtained with Eq. (1). The dynamical surface affinity index, A, is given above each fit. **(b)** Observed linear dependence of the dynamical surface affinity A with the specific surface area $S_{P,NMR}$ for the three rock-core samples.

Here $C = \pi / \left(30\, \delta_{water}^{3}\right) \sigma_S \rho_{water}\, S_{p,NMR}\, (\gamma_I \gamma_S \hbar)^2\, S(S+1)$, where $R_{1,bulk}^{water} \approx 0.4\ s^{-1}$ has no frequency dependence in the range studied [7], $S_{p,NMR}$ is the NMR specific surface area of the rock [8], $\rho_{water}=1.0\ g/cm^3$ is the water density and $\delta_{water}=0.3\ nm$ is the water molecular size. ω_I and $\omega_S=659\omega_I$ are the proton and electronic Larmor frequencies, respectively and γ_I and $\gamma_S=659\ \gamma_I$ are the gyromagnetic ratio of proton and electronic spins, respectively. The translational correlation time, τ_m, is associated with individual molecular jumps in proximity or on the surface. The surface residence time, τ_s ($>>\tau_m$), which is limited by the molecular desorption from the thin surface layer of the order of δ_{water}, controls how long the proton species *I* and *S* stay correlated at the pore surface. As we have measured by calibrated ESR the values of σ_s for the different samples we vary only the specific surface area $S_{p,NMR}$ and the two correlation times τ_m and τ_s in the best fits displayed on Fig. 4a. The values obtained for these parameters are *{0.65, 0.23, 0.12 m^2/g}* for $S_{p,NMR}$, *{0.98, 0.85, 0.87 ns}* for τ_m and *{15.7, 6.65, 2.09 μs}* for τ_s for the three rock cores *(S40, S50* and *S122)*, respectively.

Traditional techniques able to map wettability in the field are still not developed. Measurements on cores require long and tedious preparation and never reflect the actual state of wettability. These cores are generally not tested in their native state. They are cleaned and saturated with known brine and oil. They are aged and tested in spontaneous drainage (oil in water saturated core) and imbibition (water in oil saturated core). An Amott index is then determined (from *1* for water-wet rocks to -1 for oil wet cores) [9]. Another contingent method uses pressure gradient to force the flow of oil in the core saturated with water and reciprocally to force the flow of water in the core saturated with oil [10]. It gives another index called USBM (varying for $-\infty$ to $+\infty$) based on the logarithm of the ratio of energy required to move oil with water versus the energy required to move water with oil. Both Amott and USBM methods are accepted as a standard by industry; however, they do not completely compare in all cases [11]. None of these techniques allow the local probing of interaction between the fluid and the rock pore surface in a single non-invasive measurement. We have thus introduced a microscopic dynamical surface affinity, $A=\tau_s/\tau_m$, in lieu of the more traditional defined macroscopic wettability indices [1]. This index *A* is measured by a non-invasive NMR technique that represents roughly the average number of diffusing steps of spins *I* in proximity to fixed paramagnetic sites *S* during the time scale of a NMRD measurement. The larger this index, the more numerous the *2D* reencounters are, and therefore the more correlated the *I-S* spins are. This gives the dynamical surface affinity indices (NMR wettability): *A={16020, 7823* and *2402}* for the three rock cores *(S40, S50* and *S122)*, respectively (Fig. 4a). It is interesting to note the quasi linear dependence observed between the dynamical surface affinity *A* and the specific surface area $S_{p,NMR}$ (Fig. 4b). This dependence shows that the NMR wettability depends critically on the pore sizes.

4. Characterization of Dynamics of Crude Oil/Brine mixings

NMR relaxation in fluids is sensitive to molecular motions, which in turn depends on the size of the molecules and their mutual interactions. Crude oils are complex mixtures of molecules with a large range of molecular sizes which yields a broad range of relaxation times and correlation times [2-5]. Moreover, there is generally a definite amount of water (brine) mixed with these crude oils that is important to probe accurately with a non-invasive method. We propose here two NMR methods to separate the contributions of these two different petroleum fluids in a stable mixing at equilibrium without stirring.

The first NMR method is the FFC technique due to the sensitivity of the NMRD for probing different time scales of motion. The inverse Laplace fit of the longitudinal magnetization decays obtained for different mixings of crude oil/brine at each frequency gives a broad T_1-distribution that can be de-convoluted as a trimodal lognormal peak function with

diffusion-fundamentals.org 22 (2014) 5, pp 1-7

three components *(1, 2, 3)*. We present in Fig. 5a, some examples of the quasi logarithmic NMRD data of individual crude oil (sample A of components A*1, A2, A3*) and brine (sample *C*) as well as various mixings of crude oil with brine of components (*AC1, AC2, AC3)* that allows separating the different contributions in the crude oil/brine mixing. The NMRD profile of brine is a constant around 0.3 s^{-1} (Fig. 5b). We show in Fig. 5b that it is possible to reproduce the main relaxation features of the observed NMRD profiles with an equal proportion of oil and brine. The calculated proton oil NMRD in Fig. 5b have been obtained with Eq. 1 now corresponding to an intermittent surface dynamics of light oil species of density $\rho_{oil}=0.85\ g/cm^3$ and average molecular size $\delta_{oil}=0.655\ nm$ (octane) at the surface of asphaltene nanoaggregates [3]. Though the asphaltene content of the crude oils is not known, we can reasonably compare the observed (Fig. 5a) and calculated (Fig. 5b) NMRD profiles with a *2-D* translational diffusion correlation time $\tau_m=4\ ns$ and residence time $\tau_s=0.85\ \mu s$. τ_m appears to be smaller than the ones found in our previous observations on crude oil with 9 wt % of asphaltene [3], thus revealing a much lower, but present, asphaltene content.

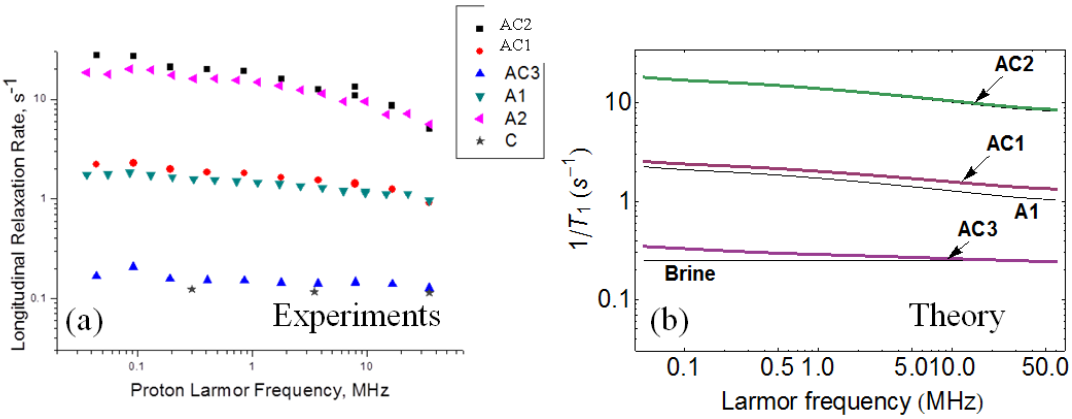

Fig. 5 (a) NMRD profiles of the relaxometric components (1, 2, 3) deduced by the fitting of the magnetization decays in a mix of crude oil (sample A) and a brine (C), compared with the individual samples separated. They are coded as: Crude-oil (A); Brine (C); Mix crude-oil + Brine (AC). (b) Theoretical NMRD of crude oil and. brine with an equation similar to Eq. (1) and parameters given in ref. [3].

The second NMR method for separating oil and brine in a crude oil/brine mixing is the *2D* T_1–T_2 correlation experiment. It is known that in multi-component systems there is potentially an exchange of proton magnetization between the various proton pools. This can occur by proton exchange and dipolar cross relaxation which introduces exchange cross-peaks into the *2D* T_1–T_2 spectrum. The extension to two dimensions has succeeded in resolving many more

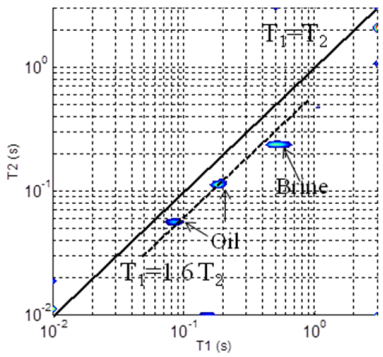

Fig. 6 *2D* T_1-T_2 correlation map of an equal mixing of bulk water and crude oil pools realized at 30 MHz

peaks [12]. Here we show on Fig. 6 the *2D* T_1-T_2 plots of an equal mixing of bulk water and crude oil performed on variable free wide-bore cryogen-free superconducting magnet. This *2D* T_1-T_2 plot has been obtained with a self-written *Matlab* program using a *2D ILT* containing a compression of the data obtained with the singular value decomposition of the two exponential kernels and a robust optimization method using a Tikhonov regularization [13, 14]. The very good signal-to-noise ratio allows limiting the artifact peaks on the edges of the map. The *2D* plot does not reveal any exchange between the different pools. In Fig. 6, the line $T_1=T_2$ is expected for a standard *3-D* bulk liquid. The observed data are aligned along a line $T_1=1.6\ T_2$ typical of a surface interaction. The only surface present here being the ones of asphaltene nanoaggregates, this confirms our previous interpretation of an intermittent surface dynamics of light oil species at the surface of asphaltene nanoaggregates [3]. The two short T_1 values *(0.085* and *0.19 s)* correspond to the two components of the crude oil at 30 MHz (see Fig. 5a). The longest $T_1=0.55\ s$ is typical of the brine value embedded in the crude oil. The quantitative analysis of the peak intensities thus gives information on the identical relative populations of the two fluids.

5. Conclusion

Multi-frequency NMR techniques have proven useful for estimating the complex multi-dynamics of bulk and confined petroleum fluids. The comparison of the observed NMRD profiles with a previously proposed nuclear spin relaxation theory induced by a two dimensional diffusion of water at pore surfaces allows probing the dynamical surface affinity (microscopic NMR wettability) of water within a set of carbonate porous rock-cores of representative sizes (1 inch). We found that this dynamical surface affinity depends critically on the pore sizes. Two NMR techniques were also used to distinguish crude oil from brine in different crude oil/brine mixing. Due to the sensitivity of the NMRD for probing different time scales of motion, the FFC technique has allowed to discriminate between oil and brine NMRD data. *2D* T_1-T_2 correlation map of a mixing of bulk water and crude oil pools performed on a variable wide-bore cryogen-free superconducting magnet allows quantitative separation of mixed bulk water and crude oil. Both techniques can potentially perform this *2-D* T_1-T_2 correlation map in a large frequency range.

References

[1] J.-P. Korb, G. Freiman, B. Nicot, P. Ligneul, Phys. Rev. E80 (2009) 061601-12.
[2] L. Zielinski, M.D. Hurlimann, Energy & Fuels, 2 (2011) 5090-5099.
[3] J.-P. Korb, , A. Louis-Joseph, L. Benamsili, J. Phys. Chem. B, 117 (2013) 7002-7014.
[4] A. Kurup, M.D. Hurlimann, J.-P. Korb *et al.* Society of Petroleum Engineers-Saudi Arabian Section Annual Technical Symposium, Saudi Arabia, May 2013
[5] L. Benamsili, J.-P. Korb, G. Hamon, A. Louis-Joseph, B. Boussiere, H. Zhou, R.G. Bryant, Energy & Fuels 28 (2014) 1629-1640.
[6] J.-P. Korb, M. Whaley and R. G. Bryant, Phys. Rev. E 56 (1997) 1934;.*ibid* E 60 (1999) 3097
[7] A. Abragam, *The Principles of Nuclear Magnetism*; Clarendon Oxford, U.K. (1961).
[8] F. Barberon, J.-P. Korb, D. Petit, V. Morin, E. Bermejo, Phys. Rev. Lett. 90 (2003) 1-4.
[9] E. Amott, Trans. AIME 216 (1959), 156.
[10] E. R. T. Donaldson and P. Lorenz, SPE J. 9 (1969) 13.
[11] A. Dixit, J. Buckley, S. McDougall, and K. Sorbie, Transp. Porous Media 40, (2000) 27.
[12] P.J. McDonald, J.-P. Korb, J. Mitchell, L. Monteilhet, Phys. Rev. E 72 (2005), 011409-9.
[13] J.-P. Butler, J.A. Reeds, S.V. Dawson,SIAM J. Numer. Anal. 18 (1981) 381-397.
[14] L. Venkataramanan, Y.Q. Song, M.D. Hürlimann, IEEE Trans. Signal Process. 50 (2002) 1017-1026.